

# 8 Fracture

## 8.1 Mode III cracks

*Fracture* describes the behaviour of thin *cracks*, like the one illustrated in Figure 8.1, in an otherwise elastic material. The crack itself is a thin void, whose faces are usually assumed to be stress-free. The simplest configuration is that of a crack in antiplane strain, which is called a Mode III crack, as illustrated in Figure 8.2. Although this configuration is not so important in practice, it is much simpler mathematically than Mode I and II cracks, which will be introduced later.

We will consider a planar crack whose faces lie close to the  $(x, z)$ -plane between the crack tips  $x = \pm c, y = 0$ . The physical set-up is that of a large cracked slab being sheared at infinity in the  $(y, z)$ -plane with a shear stress  $\sigma_{III}$ . Assuming that the faces of the crack are stress free, we find that the mathematical model for the displacement  $w(x, y)$  in the  $z$ -direction is

$$\nabla^2 w = 0 \quad (8.1a)$$

everywhere except on  $y = 0, |x| < c$ , with

$$\mu \frac{\partial w}{\partial y} \rightarrow \sigma_{III} \quad \text{as} \quad x^2 + y^2 \rightarrow \infty, \quad (8.1b)$$

$$\mu \frac{\partial w}{\partial y} = 0 \quad \text{on} \quad y = 0, |x| < c. \quad (8.1c)$$

There is a fundamental difference between (8.1) and most of the boundary value problems we have thus far considered for elastostatics, namely that the boundary on which the Neumann data (8.1c) are prescribed is not smooth at the crack tip. To see the kind of difficulty that this can cause, suppose we were to shift the origin to  $(-c, 0)$  and concentrate on the region near the crack tip. Then we would need to find a displacement field in which  $\nabla^2 w = 0$  everywhere except on  $y = 0, x > 0$ , with

$$\mu \frac{\partial w}{\partial y} = 0 \quad \text{on} \quad y = 0, x > 0. \quad (8.2)$$

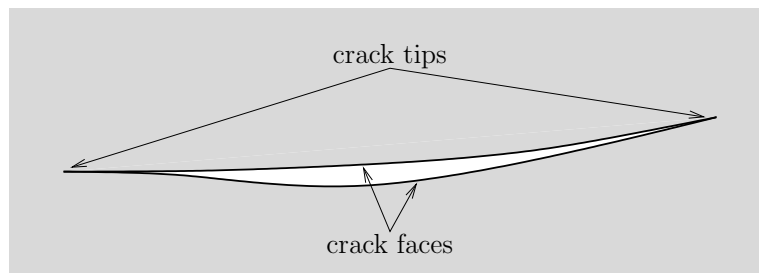


Figure 8.1: Definition sketch of a thin crack.

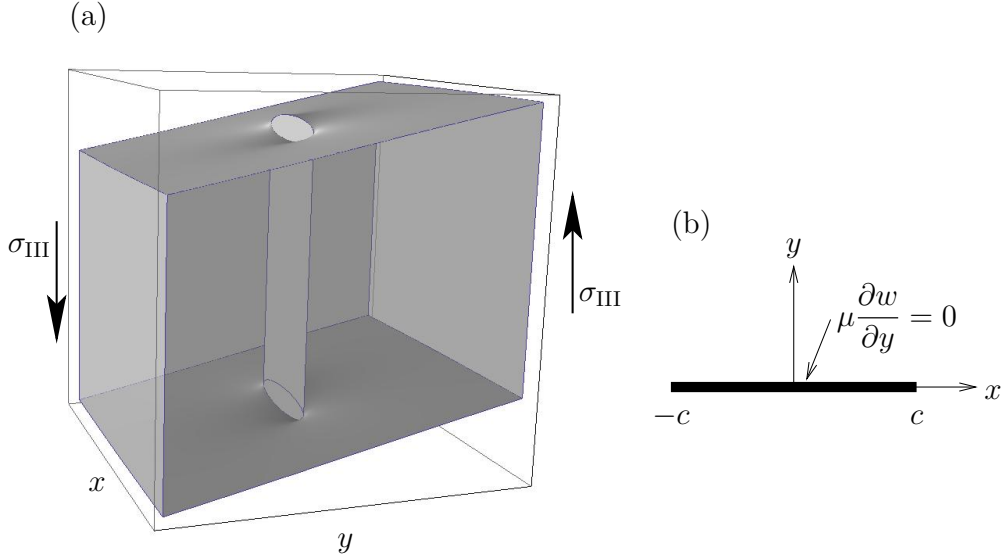


Figure 8.2: (a) A Mode III crack. (b) The cross-section in the  $(x, y)$ -plane.

By separating the variables in polar coordinates  $(r, \theta)$ , we immediately see that  $w$  can be any function of the form

$$w = Ar^{n/2} \cos(n\theta/2) = A \operatorname{Re} \left( z^{n/2} \right), \quad (8.3)$$

where  $z = re^{i\theta}$ ,  $A$  is a constant and  $n$  is an integer. The corresponding stress components are given by

$$\tau_{rz} = \frac{\mu n A}{2} r^{n/2-1} \cos(n\theta/2), \quad \tau_{\theta z} = -\frac{\mu n A}{2} r^{n/2-1} \sin(n\theta/2). \quad (8.4)$$

This plethora of solutions gives us the strong hint that we will not be able to solve (8.1) uniquely unless we supply some extra information about the behaviour of  $w$  near  $(\pm c, 0)$ . We also note that, whenever  $n$  is not an even positive integer, the stress is non-analytic at the crack tip  $r = 0$ , and, if  $n < 2$ , the stress is not even bounded.

From a mathematical point of view it is natural to ask whether the solution of (8.1) must be singular at  $(\pm c, 0)$  and, if so, what is the mildest singularity which we have to endure. To answer these questions, one possibility is to round off the crack, that is, to replace it with a thin but smooth boundary. A particularly convenient shape is the ellipse

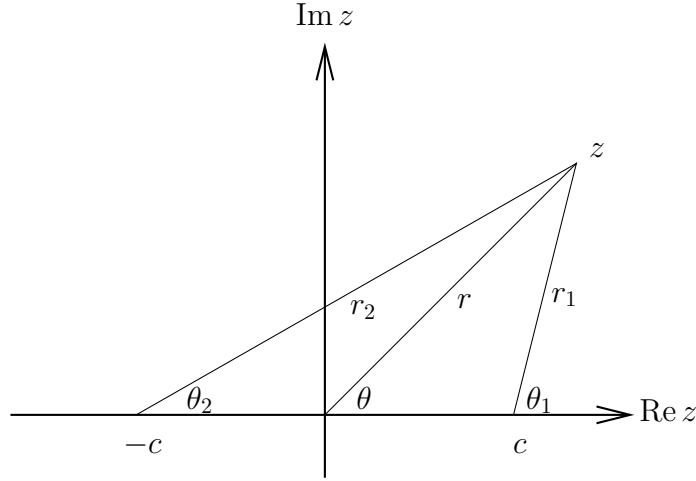
$$\frac{x^2}{c^2 \cosh^2 \varepsilon} + \frac{y^2}{c^2 \sinh^2 \varepsilon} = 1, \quad (8.5)$$

which is smooth for all positive  $\varepsilon$  but approaches the slit geometry of Figure 8.2(a) in the limit  $\varepsilon \rightarrow 0$ . Now we can easily solve Laplace's equation by introducing *elliptic coordinates* defined by

$$z = x + iy = c \cosh \zeta, \quad \text{where } \zeta = \xi + i\eta, \quad (8.6a)$$

so that

$$x = c \cosh \xi \cos \eta, \quad y = c \sinh \xi \sin \eta. \quad (8.6b)$$

Figure 8.3: Definition sketch for the function  $\sqrt{z^2 - c^2}$ .

Since the map (8.6) from  $z$  to  $\zeta$  is conformal except on  $y = 0$ ,  $|x| < c$ , Laplace's equation is preserved and the model (8.1) becomes

$$\frac{\partial^2 w}{\partial \xi^2} + \frac{\partial^2 w}{\partial \eta^2} = 0, \quad \text{in } \xi > \varepsilon \quad (8.7a)$$

with

$$\frac{\partial w}{\partial \xi} = 0 \quad \text{on } \xi = \varepsilon, \quad (8.7b)$$

and, since  $y \sim (c/2)e^\xi \sin \eta$  as  $\xi \rightarrow \infty$ ,

$$w \sim \frac{c\sigma_{\text{III}}}{2\mu} e^\xi \sin \eta \quad \text{as } \xi \rightarrow \infty. \quad (8.7c)$$

By separating the variables, we easily find the solution

$$w = \frac{c\sigma_{\text{III}}}{2\mu} \sin \eta \left( e^\xi + e^{2\varepsilon - \xi} \right). \quad (8.8)$$

We thus have a unique displacement field for any positive value of  $\varepsilon$  and, when we let  $\varepsilon \rightarrow 0$ , we obtain the solution of the crack problem as

$$w = \frac{c\sigma_{\text{III}}}{\mu} \text{Im}(\sinh \zeta). \quad (8.9)$$

Using (8.6), this can be written as

$$w = \frac{\sigma_{\text{III}}}{\mu} \text{Im} \left( \sqrt{z^2 - c^2} \right), \quad (8.10)$$

where the square root is defined to be

$$\sqrt{z^2 - c^2} \equiv \sqrt{r_1 r_2} e^{i(\theta_1 + \theta_2)/2}, \quad (8.11)$$

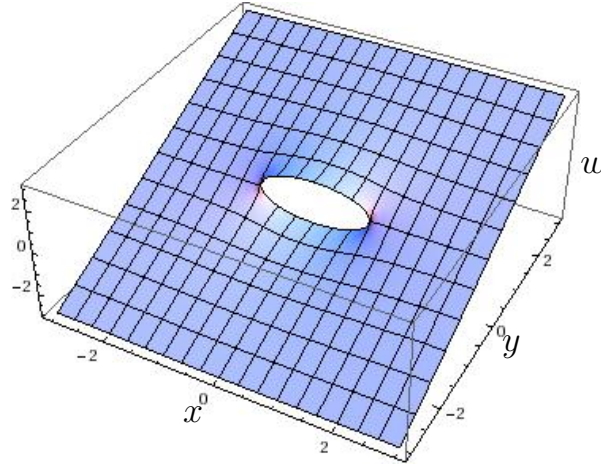


Figure 8.4: Displacement field for a Mode III crack.

with  $r_1, r_2, \theta_1$  and  $\theta_2$  defined as shown in Figure 8.3. The angles are taken to lie in the ranges  $-\pi < \theta_j < \pi$ , so that a branch cut lies along the crack between  $z = -c$  and  $z = c$ . As shown in Figure 8.4, the displacement  $w$  is discontinuous across this branch cut.

Equation (8.10) reveals the famous *square root singularity* in which the elastic displacement varies as the square root of the distance from the crack tip. By rounding off the crack before taking the limit  $\varepsilon \rightarrow 0$ , we have managed to select one of the many possible singular solutions suggested by (8.3). This dependence immediately implies that the stress tensor, whose non-zero components are

$$\tau_{xz} = \mu \frac{\partial w}{\partial x} \quad \text{and} \quad \tau_{yz} = \mu \frac{\partial w}{\partial y}, \quad (8.12)$$

diverges as the *inverse* square root of the distance from the tip. Hence *any* critical yield stress, no matter how large, will always be attained sufficiently close to the crack tip, and there must be a neighbourhood of the tip where our linear elastic model breaks down.

In the material ahead of the crack tip  $(c, 0)$ , the only non-zero stress component at the crack plane  $y = 0$  is  $\tau_{yz}$ , which satisfies

$$\lim_{x \downarrow c} \tau_{yz}(x, 0) \sqrt{x - c} = \sigma_{\text{III}} \sqrt{c/2}. \quad (8.13)$$

Hence, no matter which physical mechanism prevents the stress from becoming infinite in practice, it will have to be triggered by a local stress intensification that is proportional to the inverse square root of distance from the tip. Every Mode III crack tip is characterised by the limit defined in (8.13) and, conventionally, this limit is written as

$$\lim_{x \downarrow c} \tau_{yz}(x, 0) \sqrt{x - c} = \frac{K_{\text{III}}}{\sqrt{2\pi}}. \quad (8.14)$$

The *stress intensity factor*  $K_{\text{III}}$  is the parameter that characterises the propensity of the crack to propagate. For the crack modelled by (8.1), for example, we find that  $K_{\text{III}} = \sqrt{\pi c} \sigma_{\text{III}}$ . We postulate that the crack will propagate if  $K_{\text{III}}$  exceeds a critical value, which must be determined either from more detailed modelling of the crack tip or from experiment.

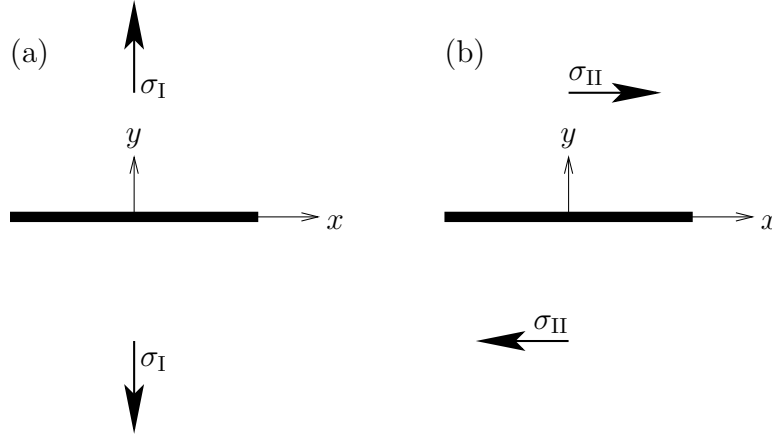


Figure 8.5: (a) Schematic of a Mode I crack. (b) Schematic of a Mode II crack.

Under this postulate, (8.13) immediately reveals that a Mode III crack is more likely to grow if it is longer or subject to greater stress. We emphasise that  $K_{III}$  is the *only* piece of information concerning the global stress field that is relevant for deciding whether or not the crack propagates.

## 8.2 Other crack geometries

More realistic than Mode III cracks are the configurations illustrated in Figure 8.5 and referred to as Mode I and Mode II cracks. The former refers to a planar crack subject to a transverse tensile stress  $\sigma_I$ , while in the latter a far-field shear stress  $\sigma_{II}$  parallel to the plane of the crack is applied. These can both be modelled using plane strain, and their analysis is inevitably more complicated than antiplane strain since we have to solve the biharmonic equation rather than Laplace's equation. Nevertheless, it can be shown that the displacement in either case varies like the square root of the distance from a sharp crack tip and, hence, that the stress diverges like the inverse square root, as it does in Mode III cracks. Thus we can define two further stress intensity factors  $K_I$  and  $K_{II}$  using formulae analogous to (8.14). A general planar crack in two space dimensions will experience a linear superposition of Modes I, II and III, and hence the stress near its tip will be characterised by three intensity factors; unfortunately there are no general rules about the Modes to which it will be most vulnerable.

Finally, we note that all the discussion hitherto refers to models of cracks that are static or just about to grow. If we wish to model a growing crack, we have to solve the *dynamic* Navier equation in a crack geometry, which is in general a difficult task. We therefore restrict our attention to the simplest possible model for a semi-infinite Mode III crack propagating at constant speed  $-V$  along the  $x$ -axis, so its tip is at  $x = -Vt$ . We can seek a travelling-wave solution moving with speed  $-V$ , at least on so the local displacement satisfies

$$\left(1 - \frac{V^2}{c_s^2}\right) \frac{\partial^2 w}{\partial \xi^2} + \frac{\partial^2 w}{\partial y^2} = 0, \quad (8.15a)$$

everywhere except on  $y = 0$ ,  $\xi > 0$ , with

$$\mu \frac{\partial w}{\partial y} = 0 \quad \text{on } y = 0, \xi > 0, \quad (8.15b)$$

where  $\xi = x + Vt$  and  $c_s$  is the shear wave speed. Notice that this problem generalises the static semi-infinite Mode III crack problem considered in (8.2).

To close the model (8.15), we should impose some conditions at infinity, but this would require us to solve for the stress away from the crack. Even without precise knowledge of this far field, we expect the physically relevant solution to have a square-root singularity analogous to (8.3) with  $n = 1$ . The corresponding solution of (8.15) is

$$w = A \operatorname{Re} \left( \sqrt{\frac{\xi}{B} + iy} \right), \quad \text{where } B^2 = 1 - \frac{V^2}{c_s^2}, \quad (8.16)$$

and it is only through the constant  $A$  that the global stress field is felt. Now the stress intensity factor is

$$K_{\text{III}} = \mu \sqrt{2\pi} \lim_{\xi \uparrow 0} \left( \sqrt{-\xi} \frac{\partial w}{\partial y}(\xi, 0) \right) = \mu A \sqrt{\frac{\pi B}{2}} = \mu A \sqrt{\frac{\pi}{2}} \left( 1 - \frac{V^2}{c_s^2} \right)^{1/4}. \quad (8.17)$$

Hence, provided  $A$  is bounded, we see that the stress intensity factor tends to zero as the tip speed tends to the shear wave speed. This is comforting because, unless cracks are boosted by internal pressures or other local driving mechanisms, they are always observed to propagate subsonically.